

Monolayers of Amphiphilic Block Copolymers via Physisorbed Macroinitiators

Torsten Stöhr and Jürgen Rühe*

Max-Planck-Institute for Polymer Research, P.O. Box 3148, 55021 Mainz, Germany

Received July 20, 1999; Revised Manuscript Received January 18, 2000

ABSTRACT: The synthesis of block copolymer monolayers at the surface of silicon oxide is described. Physisorbed monolayers of poly(ϵ -caprolactone) macroinitiators containing azo groups are used to start the radical chain polymerization of *n*-alkyl methacrylates in situ leading to the formation of amphiphilic surface-attached block copolymers. The characterization of the attached layers by surface plasmon spectroscopy, ellipsometry, infrared techniques, X-ray reflectometry, and water contact angle measurements is described. The macroinitiator technique can be used to prepare hydrophobic layers on hydrophilic substrates and allows one to circumvent some major limitations of the block copolymer physisorption process, such as solubility problems of the block copolymer and intrinsic limitations of the layer thickness.

Introduction

Because of the simplicity of the process, physisorption of block copolymers from solution is a frequently used procedure to modify the surface of solid substrates.^{1–11} Such systems, usually A–B block copolymers, consist of one block (the “anchor” A) which allows attachment to the surface of the substrate and a second block (the “buoy” B) which does not strongly interact with the surface and carries the desired surface properties¹² (Figure 1a). However, several problems are inherent with such an approach.

Since it is desired that one part of the molecule has only a weak interaction with the surface and the other a strong one, the two blocks have to be rather different from a chemical point of view. This, however, renders the task of finding a suitable solvent for the physisorption process nontrivial. If the anchor block is in a selective, bad solvent environment, the block copolymer will form micelles in solution and the adsorbed surface layer itself may have a micellar structure.^{12,13} In addition, the structural equilibration in the surface-attached block copolymer will be very slow in a selective solvent. It is conceivable that in some cases the equilibrium structure may never be reached in experimental time scales, and only metastable structures will be observed.¹² In some, from a structural point of view, very interesting cases, e.g., if the two blocks have a very different solubility, it might even be possible that no solvent for the block copolymer will be found at all. If for example one block is very hydrophobic and the other strongly hydrophilic, it will be impossible to find a suitable solvent for the block copolymer. Because of these problems, the number of systems studied so far is relatively limited (e.g., polystyrene-*block*-poly(ethylene oxide),^{1–4} polystyrene-*block*-poly(2-vinylpyridine)),^{5–8} and the chemical difference between the two blocks is in many cases rather small.

A further problem of such a physisorption process is that monolayers prepared by this technique are inherently very thin with dry film thicknesses typically

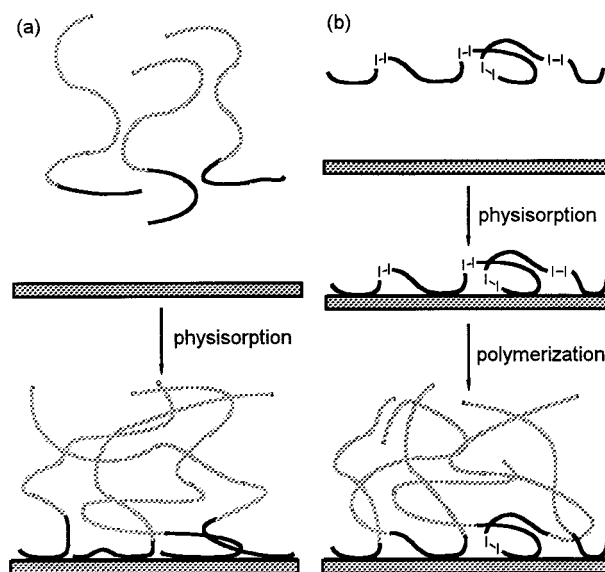


Figure 1. (a) Block copolymer adsorption from solution using a common solvent for both blocks. (b) Schematic depiction of the macroinitiator concept. The anchor block, which contains initiator groups (I–I), is physisorbed from solution to a solid surface. The buoy block is subsequently polymerized in situ.

between 30 and 50 Å. The reason for this is a kinetic hindrance for the attachment of polymer chains due to a diffusion barrier created by the already attached molecules.^{14,15}

In recent years radical polymerization using chemisorbed azo-type initiators has been developed.^{16–18} In these cases the polymer is grown directly at the surface of the substrate (“grafting-from” polymerization). The procedures described so far, however, require the presence of reactive sites at the surface of the substrate. In this work, we describe a simply physisorbed macroinitiator system that allows the creation of hydrophobic layers on hydrophilic surfaces. A hydrophilic anchor block bearing initiator groups was physisorbed to the hydrophilic surface from solution. The hydrophobic buoy block was polymerized in situ, resulting in a block copolymer monolayer (Figure 1b). Poly(ϵ -caprolactone) was used as an example for a suitable anchor block as it is known to physisorb to hydrophilic surfaces.^{19–21}

* To whom correspondence should be addressed. Phone +49–6131–379–162; fax +49–6131–379–100, e-mail ruehe@mpip-mainz.mpg.de.

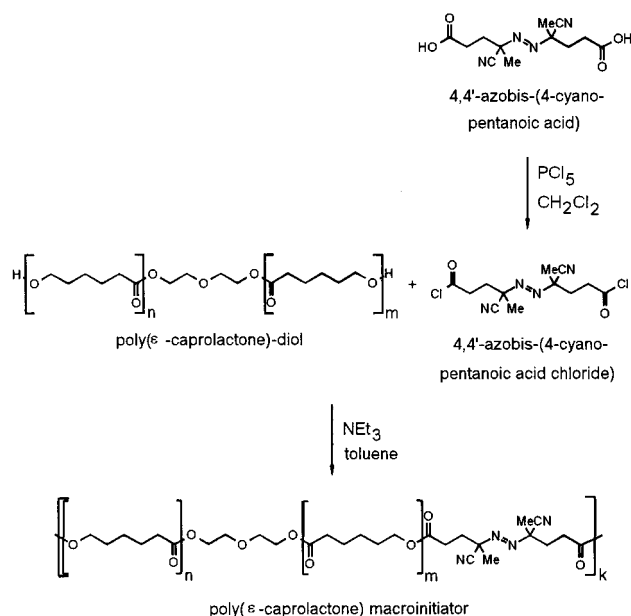


Figure 2. Synthesis of the poly(ϵ -caprolactone) macroinitiator. $P_{n,\text{PCLD}} = n + m = 13.0$ and $M_{n,\text{PCLD}} = 1590$ g/mol for the poly(ϵ -caprolactone)diol. $P_{n,\text{PCLM}} = 2k = 10.1$ and $M_{n,\text{PCLM}} = 9250$ g/mol for the poly(ϵ -caprolactone) macroinitiator.

Thus, an oligomeric poly(ϵ -caprolactone) macroinitiator containing azo moieties was synthesized and adsorbed to silicon oxide surfaces. The surface-attached monolayer was subsequently used for free radical chain initiation of the polymerization of *n*-alkyl methacrylates.

Experimental Section

Materials. 4,4'-Azobis(4-cyanopentanoic acid) was obtained from Fluka. Poly(ϵ -caprolactone)diol (Aldrich, melting point $\vartheta_m = 45$ °C, number-average molecular weight $M_{n,\text{PCLD}} = 1250$ g/mol according to the supplier) was repeatedly dissolved in a small volume of toluene and precipitated with a 15-fold excess of *n*-hexane in order to remove diglycol impurities. The precipitate was filtered off, washed with ethanol, and dried in a vacuum. Size exclusion chromatography (SEC) using a poly(styrene)/tetrahydrofuran (THF) calibration: apparent $M_{n,\text{PCLD}} = 1600$ g/mol, apparent polydispersity $D = M_w/M_n = 2.2$. ^1H NMR end group analysis: number-average degree of polymerization $P_{n,\text{PCLD}} = n + m = 13.0$ (Figure 2) or $M_{n,\text{PCLD}} = 1590$ g/mol. Triethylamine (NEt_3) was dried by distillation from CaH_2 . Silica powder (Aerosil A300, Degussa) was dried by heating to 110 °C at 10^{-2} mbar overnight. Its specific surface area of 285 ± 15 m²/g was determined by nitrogen adsorption measurements evaluated according to Brunauer, Emmett, and Teller (BET technique). Toluene (analytical grade) was dried by distillation from sodium using benzophenone as an indicator. Dry decalin (analytical grade) and cyclohexane (analytical grade) were used as obtained. The monomers methyl (Fluka), *n*-butyl (Polysciences), *n*-hexyl (Röhm), lauryl (Aldrich), and stearyl methacrylate (Merck) were chromatographically purified over basic alumina, distilled in vacuum from Cu(I)Cl , and stored under dry argon at -18 °C. All other chemicals were used as obtained.

Macroinitiator Synthesis. Figure 2 shows the synthesis of the poly(ϵ -caprolactone) macroinitiator. 4,4'-Azobis(4-cyanopentanoic acid chloride) was prepared by a modified literature²² procedure. A 28 g (0.10 mol) sample of 4,4'-azobis(4-cyanopentanoic acid) was carefully added to a suspension of 104 g (0.50 mol) of PCl_5 in 200 mL of CH_2Cl_2 under ice cooling. The reaction mixture was warmed to room temperature and stirred overnight. Excess PCl_5 was filtered off. The volume was reduced to 20% by evaporating CH_2Cl_2 , whereby more PCl_5 precipitated as a yellow solid, which again was filtered off. The product was isolated by slowly pouring the filtrate into

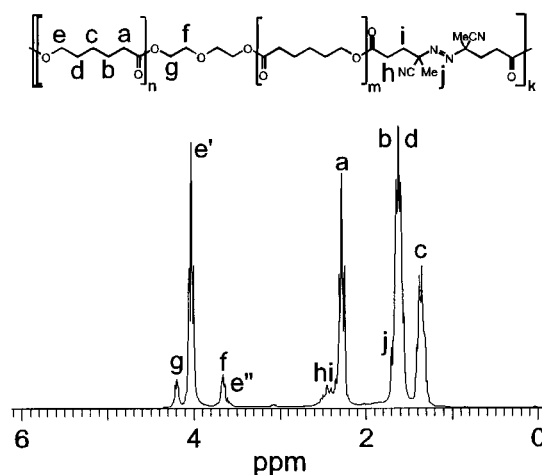


Figure 3. Peak assignment in ^1H NMR spectrum of the poly(ϵ -caprolactone) macroinitiator.

300 mL of ice-cold *n*-hexane, filtering off, washing with ice-cold *n*-hexane, and drying in a vacuum, yielding 22 g (0.07 mol, 69%, literature:²² 75%). $\vartheta_m = 91$ °C (literature:²² 102 °C by differential scanning calorimetry (DSC)). ^1H NMR (CDCl_3 , δ in ppm): 3.23–2.87 (m, 4H, CH_2CO), 2.64–2.37 (m, 4H, CH_2C), 1.72 and 1.66 (s each, 6H total, CH_3).

A solution of 3.0 g (0.0095 mol) of 4,4'-azobis(4-cyanopentanoic acid chloride) in 150 mL of dry toluene (solubility ~ 20 g/L) was slowly added to a solution of 18.6 g (0.0117 mol) of poly(ϵ -caprolactone)diol and 13.0 mL (0.0936 mol) of dry NEt_3 in 80 mL of dry toluene under vigorous stirring. The molar feed ratio was $r_f = 0.81$. After stirring for an additional hour, the hydrochloride was filtered off and the toluene was evaporated. The residue was suspended in a small volume of *n*-hexane, transferred into a suction funnel, washed with ethanol and water several times, and dried in a vacuum yielding 19.1 g (0.0021 mol, 91% referring to poly(ϵ -caprolactone)diol). DSC: $\vartheta_M = 49$ °C, $\vartheta_D = 123$ °C, $\Delta H_D = -200$ kJ/mol referring to azo groups. ^1H NMR (Figure 3, CDCl_3 , δ in ppm): 4.19 (t, 4.6 Hz, $\text{CO}-\text{O}-\text{CH}_2(\text{g})-\text{CH}_2-\text{O}$), 4.02 (t, 6.6 Hz, $\text{O}-\text{CH}_2(\text{e}')-\text{CH}_2-\text{CH}_2-\text{CH}_2-\text{CH}_2-\text{CO}$), 3.67 (t, 4.7 Hz, $\text{CO}-\text{O}-\text{CH}_2-\text{CH}_2(\text{f})-\text{O}$), 3.61 (t, 6.7 Hz, $\text{HO}-\text{CH}_2(\text{e}'')$), 2.57–2.40 (m, $\text{CH}_2(\text{h})-\text{CH}_2(\text{i})-\text{C}(\text{CN})$), 2.27 (t, 7.4 Hz, $\text{O}-\text{CH}_2-\text{CH}_2-\text{CH}_2-\text{CH}_2(\text{a})-\text{CO}$), 1.70 (s, $\text{CH}_3(\text{j})$), 1.69–1.55 (m, $\text{O}-\text{CH}_2-\text{CH}_2(\text{d})-\text{CH}_2-\text{CH}_2(\text{b})-\text{CH}_2-\text{CO}$), 1.40–1.29 (m, $\text{O}-\text{CH}_2-\text{CH}_2-\text{CH}_2(\text{c})-\text{CH}_2-\text{CH}_2-\text{CO}$). SEC (poly(styrene)/THF calibration): apparent $M_{n,\text{PCLM}} = 9000$ g/mol, apparent $D = 5.4$. ^1H NMR end group analysis and thermogravimetric analysis (TGA): $P_{n,\text{PCLM}} = 2k = 10.1$ (Figure 2) or $M_{n,\text{PCLM}} = 9250$ g/mol.

Macroinitiator Physisorption. The substrates were dried in vacuo at 10^{-2} mbar for 2 h. After this a solution of the poly(ϵ -caprolactone) macroinitiator in dry toluene was added through 0.2 μm filters (Millipore). After 16 h the substrates were removed from the solution and thoroughly rinsed with toluene. To remove weakly physisorbed macroinitiator, the substrates were continuously extracted in dry toluene at 15 °C for 16 h using a water-cooled Soxhlet extractor. For thermal analysis a solution of 0.5 g of macroinitiator in 100 mL of dry toluene was added to 1 g of dry silica powder. After stirring for 16 h, the centrifuged product was immersed in another 100 mL of dry toluene for 16 h to remove weakly physisorbed macroinitiator and centrifuged again.

"Grafting-From" Polymerization. Again the substrates were dried in vacuo at 10^{-2} mbar for 2 h. The chosen *n*-alkyl methacrylate and solvent were added under dry argon atmosphere in appropriate relations. The solutions were degassed in a vacuum through repeated freeze–thaw cycles and heated under vacuum to 60.0 ± 0.1 °C. The polymerizations were stopped after selected periods of time by cooling to room temperature. To remove weakly physisorbed poly(*n*-alkyl methacrylate) homopolymer, the substrates were continuously

extracted with cyclohexane at 15 °C for 16 h using a Soxhlet extractor. The exception to this were the poly(methyl methacrylate) covered samples which were extracted with dry toluene.

Bulk Characterization Methods. In the case of the poly(ϵ -caprolactone) derivatives SEC measurements were performed in THF (HPLC grade quality) using a column combination of 500, 10⁵, and 10⁶ Å pore size (styrene-divinylbenzene copolymer, Polymer Standards Service). In the case of the high molecular weight poly(*n*-alkyl methacrylates) a column combination of 10⁵, 10⁶, and 10⁷ Å pore size was used. Both were calibrated by poly(styrene) standards, the latter by standards of molecular weights up to 10⁷ g/mol (Polymer Standards Service). The latter calibration curve was converted into a poly(methyl methacrylate) curve by universal calibration using $K = 0.013\ 63\ \text{mL/g}$, $a = 0.714$ for poly(styrene) and $K = 0.0075\ \text{mL/g}$, $a = 0.72$ for poly(methyl methacrylate) in THF at 25 °C.²³ A differential refractometer (RI ERC 7512, Erma) was used for detection. Additionally, the molecular weights of the poly(*n*-alkyl methacrylates) were determined by static light scattering (Spectra Physics Kr 2025, ALV) at $\lambda = 647.1\ \text{nm}$ using THF (HPLC grade quality) as the solvent. The refractive index increments used were $dn/dc = 0.0649\ \text{mL/g}$ for poly(*n*-butyl methacrylate), $0.0669\ \text{mL/g}$ for poly(*n*-hexyl methacrylate), and $0.0680\ \text{mL/g}$ for poly(stearyl methacrylate) obtained at $\lambda = 632.8\ \text{nm}$ using a home-built Michelson interferometer.

¹H NMR spectra were recorded on a Bruker Avance 250 using CDCl₃ as the solvent. The TGA measurement was performed on a Mettler TG 50 at a scan rate of 10 °C/min. The bulk IR spectra of films cast onto NaCl plates were recorded using the Perkin-Elmer FTIR spectrometer Paragon 1000 at a resolution of 2 cm⁻¹. Refractive indices were measured with a conventional refractometer (Atago). Densities were measured using pycnometers.

Surface Characterization Methods. A Mettler DSC 30 was used to take DSC traces at a scan rate of 10 °C/min. Adsorption enthalpies were measured semiadiabatic calorimetry²⁴ (2225 solution calorimeter, Thermometric). The equipment calibration was checked by measuring the dissolution enthalpy of TRIS (tris(hydroxymethyl)aminomethane, reference material 724 of the United States National Bureau of Standards) in water at 25 °C as -29.747 kJ/mol (literature:²⁵ -29.744 kJ/mol). For these experiments an ampule containing ~1 g of a 50 wt % emulsion of the macroinitiator in dry toluene was broken under stirring within a reaction vessel containing a suspension of 1 g of dry silica powder in 100 mL of dry toluene. The product was isolated by centrifugation.

Grazing incidence FTIR spectra were recorded using a Nicolet Magna-IR 850 spectrometer series II at an incident angle of 5° and a resolution of 2 cm⁻¹. Glass slides (B270, Berliner Glas) with a 1000 Å thick Au layer and a 100 Å thick SiO_x (1 ≤ *x* ≤ 2) layer on top were used as substrates. Transmission FTIR spectra were recorded using a Nicolet 730 FTIR spectrometer at a resolution of 1 cm⁻¹. For these measurements silicon wafers (Aurel) polished on both faces and having a natural SiO_x layer of approximately 30 Å were used.

Surface plasmon spectroscopy measurements were carried out in air using the Kretschmann²⁶ configuration with an He-Ne laser ($\lambda = 632.8\ \text{nm}$). 90° prisms (BK7, $n_D^{20} = 1.5151$, Spindler & Hoyer) and index match fluid ($n_D^{20} = 1.5160$, Cargill) were used. The substrates were glass slides onto which a 500 Å thick Ag layer and a 300 Å thick SiO_x layer had been evaporated. Layer thicknesses were determined according to Fresnel equations.

Small-angle X-ray reflectometry measurements were carried out with a 18 kW Rigaku rotating anode in $\theta/2\theta$ geometry using the K α radiation from a copper target ($\lambda = 1.518\ \text{\AA}$).²⁷ Polished silicon wafers (Aurel) with a natural SiO_x layer of approximately 30 Å were used as substrates. The data were evaluated by fitting them to curves calculated from a layer model using an optical matrix formalism.²⁸ Since the SiO_x layer could not be distinguished from the silicon due to the matching electron densities and since the low thickness of the initiator

monolayer made a separate fit meaningless, the model was reduced to a simple three-layer system consisting of the substrate Si/SiO_x, the polymer layer, and air. The shape of the interface polymer/air was modeled by an error function whose parameter σ described the rms roughness of the polymer layer. The fitting process was allowed to vary thickness, electron density, and roughness of the polymer film. The electron density and the roughness of the substrate Si/SiO_x had been derived separately.

Ellipsometry (EL X-1, Dr. Riss Ellipsometerbau) was used to determine film thicknesses on silicon wafers. Water contact angle measurements were performed with a contact angle microscope (Krüss) using ultrapure water (Milli-Q Plus 185, Millipore).

Results and Discussion

Macroinitiator Synthesis. The poly(ϵ -caprolactone) macroinitiator was prepared by polycondensation of 4,4'-azobis(4-cyanopentanoic acid chloride) with poly(ϵ -caprolactone)diol (Figure 2). Since high molecular weight poly(ϵ -caprolactone) macroinitiator was only marginally soluble or even insoluble in common organic solvents, low molecular weight polymer was synthesized by adjusting the molar feed ratio of 4,4'-azobis(4-cyanopentanoic acid chloride) to poly(ϵ -caprolactone)diol. In the case described in the following it was chosen as $r_f = 0.81$. The molar composition r_c of the two monomers was determined by ¹H NMR end group analysis as well as TGA.

In the ¹H NMR spectra of the poly(ϵ -caprolactone)diol the integrals ($g + e' + f + e''$) and a can easily be determined. (For definition of the integrals see Figure 3 and Experimental Section.) The number-average degree of polymerization of the poly(ϵ -caprolactone)diol $P_{n,\text{PCLD}}$ was derived according to

$$P_{n,\text{PCLD}} = \frac{2a}{g} = \frac{4a}{(g + e' + f + e'') - a} \quad (1)$$

Thus, the number-average degree of polymerization was given as $P_{n,\text{PCLD}} = n + m = 13.0$ (Figure 2), and the number-average molecular weight was calculated as $M_{n,\text{PCLD}} = 1590\ \text{g/mol}$. In a similar manner the integrals ($h + i + a$) and ($g + e' + f + e''$) can easily be determined in the ¹H NMR spectra of the poly(ϵ -caprolactone) macroinitiator. The molar composition of $r_c = 0.78$ was calculated using

$$r_c = \frac{h + i}{g + f} = \frac{(h + i + a) - \frac{(g + e' + f + e'')}{1 + 4/P_{n,\text{PCLD}}}}{(g + e' + f + e'') \left(1 - \frac{1}{1 + 4/P_{n,\text{PCLD}}} \right)} \quad (2)$$

The composition can also be checked by TGA analysis. The step in the TGA trace of the poly(ϵ -caprolactone) macroinitiator is due to the loss of nitrogen m_{N_2} . The relative mass loss of $m_{\text{N}_2}/m_0 = 1.33\%$ was used to determine the molar composition r_c according to

$$r_c = \frac{m_{\text{N}_2}}{m_0 M_{\text{N}_2}} \left/ \frac{1 - \frac{m_{\text{N}_2}}{m_0 M_{\text{N}_2}} (M_{\text{ABAC}} - M_{\text{Cl}})}{M_{n,\text{PCLD}} - 2M_{\text{H}}} \right. \quad (3)$$

Here m_0 is the sample mass. M_{N_2} , M_{ABAC} , M_{H} , and M_{Cl} are the molar weights of a nitrogen molecule, a 4,4'-azobis(4-cyanopentanoic acid chloride) molecule, hydrogen, and chlorine, respectively. A molar composition of $r_c = 0.86$ was obtained.

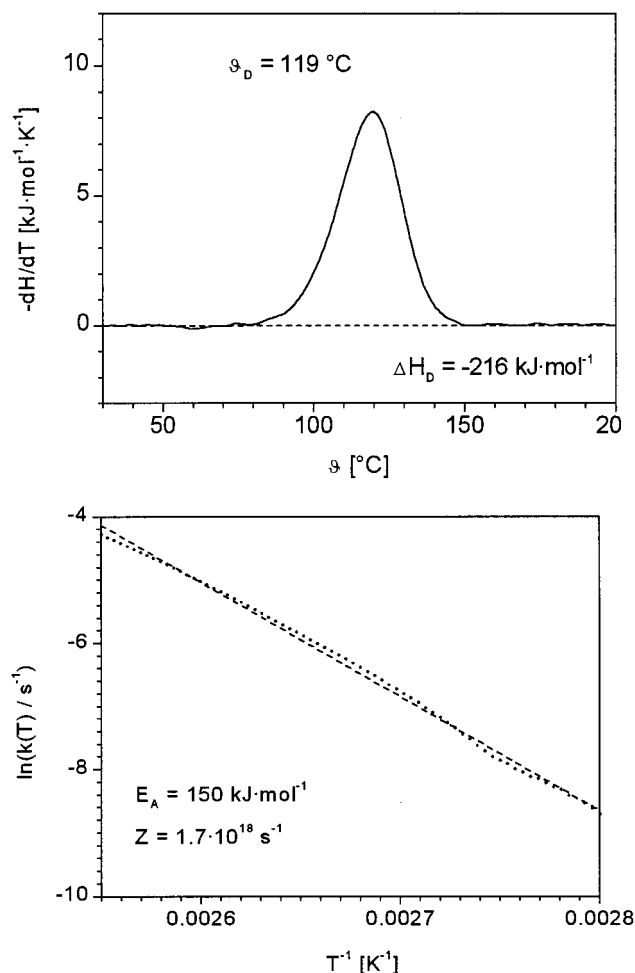


Figure 4. (a) DSC trace of the poly(ϵ -caprolactone) macroinitiator physisorbed to spherical silicon oxide powder. A layer thickness of $d_{\text{PCLM}} = 6$ Å was estimated according to eq 11. (b) Arrhenius plot calculated from the DSC trace depicted in (a).

The composition ratios derived by the two methods were averaged to $r_c = 0.82$, which is very close to the molar feed ratio $r_f = 0.81$. Furthermore, this led to a number-average degree of polymerization of $P_{n,\text{PCLM}} = 2k = 10.1$ (Figure 2) using²⁹

$$P_{n,\text{PCLM}} = \frac{1 + r_c}{1 - r_c} \quad (4)$$

From this the number-average molecular weight was calculated to be $M_{n,\text{PCLM}} = 9250$ g/mol, which is in good agreement with the apparent $M_{n,\text{PCLM}} = 9000$ g/mol derived by SEC. A ratio $r_c/P_{n,\text{PCLM}}$ of roughly 5 azo units per 80 ϵ -caprolactone repeat units is found in each initiator molecule.

Kinetics of Azo Decomposition. Since immobilization of an initiator might change the thermal decomposition behavior of the azo groups,^{30,31} the decomposition kinetics of the poly(ϵ -caprolactone) macroinitiator physisorbed to silica were investigated by DSC. In Figure 4a the DSC trace of the macroinitiator physisorbed to spherical silica powder is depicted. The activation energy of the azo decomposition was calculated according to a method developed by Nuyken³² and others.^{33,34} They have shown that the complete Arrhenius plot of the thermal decomposition of a thermally labile compound can be obtained from a single DSC trace.

If the process is assumed to be a first-order reaction, then the reaction rate $-dn(t)/dt$ is given by

$$-\frac{dn(t)}{dt} = k_D(t) n(t) \quad (5)$$

where $k_D(t)$ is the rate constant of the decomposition and $n(t)$ is the number of nondecomposed molecules at time t . Furthermore, the reaction rate is proportional to the heat flow $dH_D(t)/dt$:

$$-\frac{dn(t)}{dt} = \frac{n_0}{\Delta H_D} \frac{dH_D(t)}{dt} \quad (6)$$

where n_0 is the number of initially present initiator molecules and ΔH_D is the decomposition enthalpy. Accordingly, k_D can be expressed as

$$k_D(t) = \left(\Delta H_D \frac{n(t)}{n_0} \right)^{-1} \frac{dH_D(t)}{dt} \quad (7)$$

The last factor $dH_D(t)/dt$ can directly be read from the DSC trace for any given time t . The term $\Delta H_D n(t)/n_0$ can be derived from the integral of the DSC curve. To obtain this value, the signal has to be integrated from the beginning of the decomposition until time t and subtracted from the total amount of heat released during complete decomposition.

Figure 4b shows the Arrhenius plot based on

$$k_D(T) = Z \exp\left(-\frac{E_A}{RT}\right) \quad (8)$$

E_A represents the activation energy of the decomposition, R the universal gas constant, and Z is the preexponential factor. The values of $k_D(T)$ were derived from the DSC trace in Figure 4a via the method described above. Only the linear part of the data between 84 and 119 °C is presented. Deviations from the linear slope are observed at lower and higher temperatures. At lower temperatures the signal is too small for reliable analysis. Deviations at higher temperatures are most likely due to the accumulation of decomposition products, such as ketenimines, that can undergo further thermal reactions. From the slope of the Arrhenius plot E_A was determined to be 150 kJ/mol, which is in close agreement to the reported values for α, α' -azobis(isobutyronitrile) (AIBN:³⁵ 120–142 kJ/mol). Using the results of the Arrhenius plot, the rate constant at 60 °C, which is the temperature used for the polymerizations described below, was calculated as $k_D(60 \text{ °C}) = 4.5 \times 10^{-6} \text{ s}^{-1}$ (AIBN:³⁵ $(4.0\text{--}9.4) \times 10^{-6} \text{ s}^{-1}$). Thus, it can be concluded that the incorporation of an AIBN analogous group into the poly(ϵ -caprolactone) macroinitiator and the immobilization to silica do not have a significant influence on the thermal behavior of the azo moiety.

Macroinitiator Physisorption. To evaluate data obtained by surface plasmon spectroscopy and ellipsometry, the refractive index n_D^{20} of the poly(ϵ -caprolactone) macroinitiator has to be known. Since the macroinitiator contains only few azo units, it is safe to assume that the refractive indices of the initiator and the diol are similar. However, it should be noted that the initiator monolayers are in an amorphous state whereas the poly(ϵ -caprolactone)diol is crystalline at room temperature. The refractive index of an amorphous material was obtained from the temperature

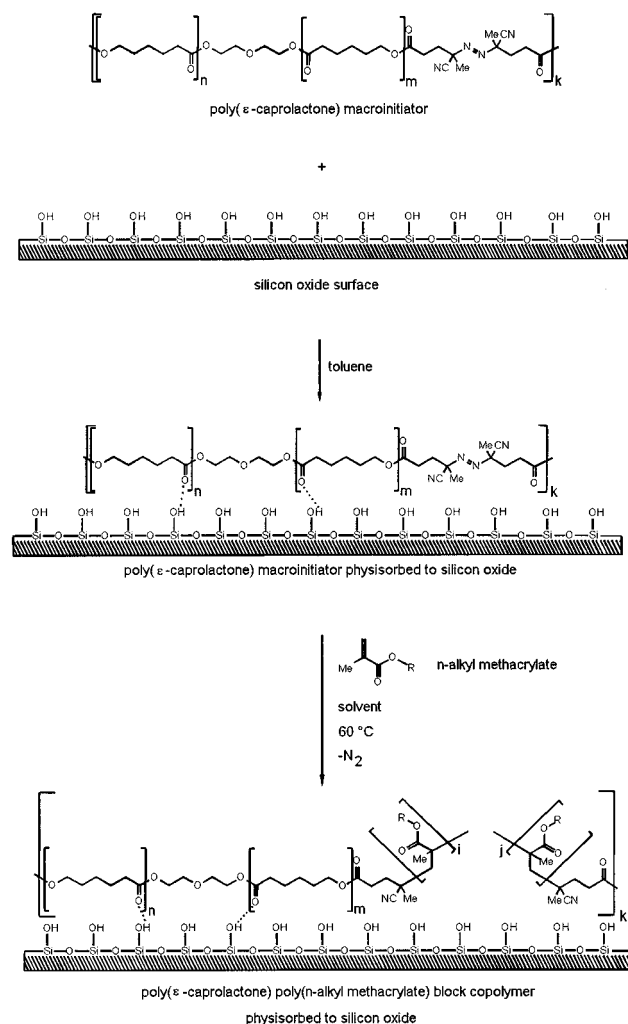


Figure 5. Physisorption and polymerization process. The physisorption of the macroinitiator is accompanied by the formation of hydrogen bonds mainly between the SiOH groups of the silicon oxide and C=O groups of the initiator. The surface polymerization leads to formation of block copolymers in situ.

dependence of the refractive index of a melt and extrapolation to room temperature as $n_D^{20} = 1.472$.

Toluene was used as a solvent for the physisorption of the poly(ϵ -caprolactone) macroinitiator onto silicon oxide. The physisorption is most likely due to the formation of hydrogen bonds between C=O groups of the initiator and the SiOH groups of the silicon oxide (Figure 5). The IR spectra shown in Figure 6a,b qualitatively prove the presence of the macroinitiator monolayer. The grazing incidence FTIR spectrum taken for a film of ~ 18 Å (see below) poly(ϵ -caprolactone) macroinitiator and the FTIR spectrum taken for a cast film are in good agreement. The shift of the $\nu(\text{C}=\text{O})$ valence vibration toward higher wavenumbers for the physisorbed macroinitiator (1737 cm^{-1}) compared to bulk macroinitiator (1723 cm^{-1}) is most likely due to the loss of crystallinity.

A basic requirement for any successful physisorption process is that the free energy of solvation of the polymer molecules is less than the free energy of adsorption. Furthermore, the latter one determines the tethering strength of the molecules to the surface which is an important parameter for many physical properties of the system. Calorimetry measurements allow the

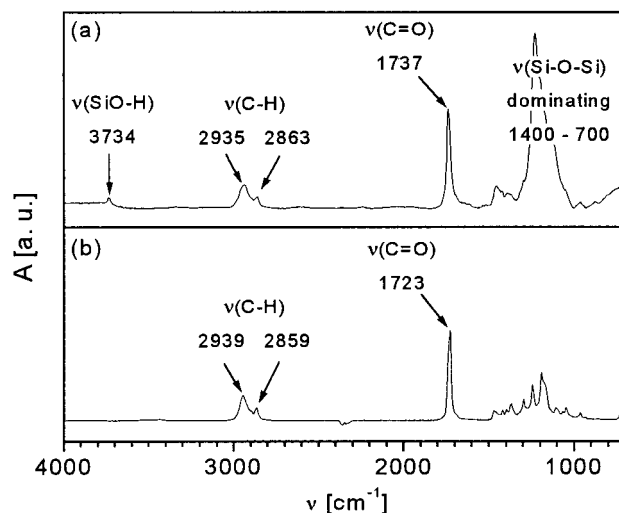


Figure 6. (a) Grazing incidence IR spectrum of a macroinitiator monolayer physisorbed to SiO_x . (b) Bulk IR spectrum of the same compound.

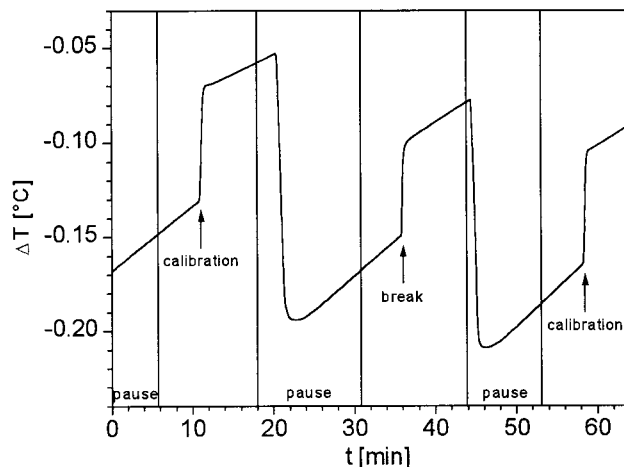


Figure 7. Calorimetric study of the adsorption process. The poly(ϵ -caprolactone) macroinitiator dissolved in toluene is added to silica powder suspended in toluene. The temperature offset ΔT is shown as a function of time t . The heat signal for the adsorption process is supplemented by two calibration runs of 10 J each. Further details are described in the text.

determination of the enthalpy of adsorption directly. To observe reliable heat effects, a concentrated (50 wt %) solution or—to be more precise as not all macroinitiator dissolved—an emulsion containing an initial amount m_0 of poly(ϵ -caprolactone) macroinitiator in toluene was filled into the ampule. After breaking the ampule in a suspension of silica powder in toluene, a temperature offset ΔT is observed as depicted in Figure 7. The adsorption enthalpy ΔH_A results from the subtraction of the dilution enthalpy from the measured heat effect ΔH_M :

$$\Delta H_A = \Delta H_M - m_0 \Delta H_{D,\text{spec}} \quad (9)$$

Here $\Delta H_{D,\text{spec}}$ is the specific dilution enthalpy that was obtained by repeating the experiment without the presence of silica. The dilution process was found to be endothermic with an enthalpy of $\Delta H_{D,\text{spec}} = 1.3\text{ J/g}$. The adsorbed amount m_A was determined by weighing the dried sol and gel phases. This allowed to determine the specific adsorption enthalpy $\Delta H_{A,\text{spec}}$. Additionally, since C=O groups within the ϵ -caprolactone unit and further

Table 1. Calorimetric Study of the Adsorption of the Poly(ϵ -caprolactone) Macroinitiator to Silica Powder from Toluene Solution at 25 °C

run	m_0 [g]	ΔH_M [J]	ΔH_A [J]	m_A [g]
1	0.489	-8.39	-9.04	0.269
2	0.310	-7.03	-7.45	0.211

run	$\Delta H_{A,spec}$ [J/g]	$\Delta H_{A,mol}$ [kJ/mol]	d_{PCLM} [Å]	c_{ARU} [mol/L]
1	-33	-4.1	8	0.018
2	-35	-4.3	7	0.008

C=O groups within azo moiety as well as oxidic groups within the diglycol have to be taken into account as adsorption sites, a molar adsorption enthalpy $\Delta H_{A,mol}$ was derived using the molecular weight M_{ARU} of an average repeat unit as defined by

$$M_{ARU} = \frac{P_{n,PCLD}M_{CL} + (M_{DG} - 2M_H) + (M_{ABAC} - M_{Cl})}{P_{n,PCLD} + 2} \quad (10)$$

where $P_{n,PCLD}$ is the number-average degree of polymerization of the poly(ϵ -caprolactone)diol and M_{CL} , M_{DG} , M_H , M_{ABAC} , and M_{Cl} are the molar weights of an ϵ -caprolactone repeat unit, a diglycol molecule, hydrogen, a 4,4'-azobis(4-cyanopentanoic acid chloride) molecule, and chlorine, respectively. The thickness d_{PCLM} of the poly(ϵ -caprolactone) macroinitiator physisorbed to spherical silica particulates was estimated by

$$d_{PCLM} = \frac{m_A}{\rho_{PCLM}A} \quad (11)$$

where A is the surface area of 1 g of silica powder and ρ_{PCLM} is the density of the poly(ϵ -caprolactone) macroinitiator. The latter was assumed to be similar to the density of poly(ϵ -caprolactone)diol and was determined to be 1.122 g/cm³ by means of conventional pycnometry. Additionally, the equilibrium solution concentration of average repeat units c_{ARU} was estimated by

$$c_{ARU} = \frac{m_0 - m_A}{M_{ARU}V} \quad (12)$$

where V is the reaction volume.

The specific adsorption enthalpy is derived as $\Delta H_{A,spec} = -34$ J/g and $\Delta H_{A,mol} = -4.2$ kJ/mol (referring to average repeat units) as shown in Table 1. These values are about a factor of 3 smaller than $\Delta H_{A,spec} = -111$ J/g and $\Delta H_{A,mol} = -12.7$ kJ/mol, respectively, which were determined for the physisorption of a poly(ϵ -caprolactone) homopolymer of $M_n = 10\,700$ g/mol to silica powder from a CCl₄ solution.¹⁹ This difference can on one hand be attributed to the better solvent quality of toluene compared to CCl₄ and on the other hand to the less regular structure of the poly(ϵ -caprolactone) macroinitiator monolayer compared to the homopolymer monolayer. Generally, the obtained values show that the polymeric initiators are strongly tethered to the substrate.

Surface plasmon spectroscopy measurements (Figure 8) of samples before and after toluene extraction show that some part of the macroinitiator layer is only weakly physisorbed and can be removed by the extraction process. However, some part of the monolayer is strongly physisorbed and remains attached to the silicon oxide

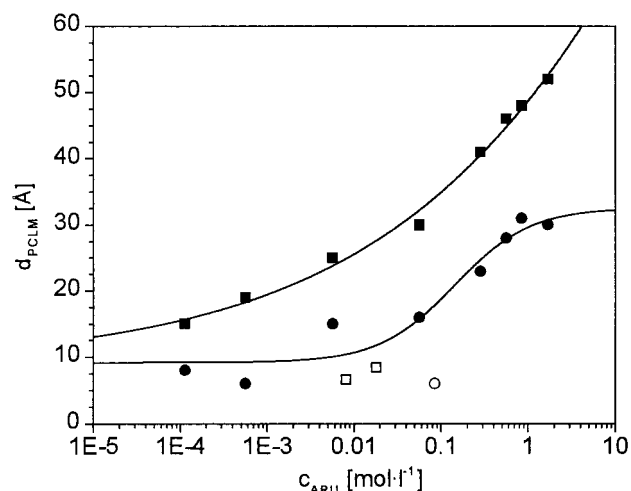


Figure 8. Layer thickness of the poly(ϵ -caprolactone) macroinitiator monolayers d_{PCLM} determined by surface plasmon spectroscopy as a function of the solution concentration c_{ARU} . Measurements are shown directly after physisorption from toluene for 16 h and simple rinsing (■) and after extraction with toluene for 16 h (●). In addition, the nonextracted layer thicknesses which were calculated from the adsorbed amount after the calorimetric measurements (□) and the layer thickness on polished silicon wafers after extraction (○) are indicated.

surface even after prolonged extraction. The thickness d_{PCLM} of the strongly physisorbed poly(ϵ -caprolactone) macroinitiator layer is a function of the solution concentration c_{ARU} from which it is physisorbed. Toward very high concentrations the layer thickness of the initiator reaches a plateau value. Here the maximum number of SiOH adsorption sites on the substrate have built up hydrogen bonds to the C=O groups of the macroinitiator limiting the layer thickness. At very low concentrations a constant minimum thickness is observed which is attributed to molecules in an extremely flat, pancake-like conformation with a high amount of adsorption sites per molecule.

Furthermore, the type of substrate used for adsorption also influences the obtainable macroinitiator layer thickness d_{PCLM} . The thicknesses obtained on spherical silica powder (Table 1) reflect thicknesses of nonextracted layers which have to be compared to the thicknesses of nonextracted layers obtained on the planar substrates having a layer of evaporated SiO_x on top (Figure 8). The former are considerably lower than the latter which is most likely due to an error in the surface area of the evaporated SiO_x. All calculations were based on the geometrical surface area of the planar substrate while the true surface area is significantly higher due to the surface roughness. This interpretation of the thickness values agrees well with the results on polished silicon wafers which are much smoother than the evaporated SiO_x and on which also lower thicknesses were obtained. Extracted thicknesses of $d_{PCLM} = 6 \pm 2$ Å (Figure 8) on polished silicon wafers and of $d_{PCLM} = 18 \pm 6$ Å on evaporated SiO_x were obtained for monolayers adsorbed from a $c_{ARU} = 0.085$ mol/L solution which was chosen as the standard concentration for further experiments.

The initial azo surface density $\Gamma_{azo,0}$ within the initiator monolayer is an important parameter for surface polymerization reactions. Knowing d_{PCLM} , the initial density $\Gamma_{azo,0}$ could be calculated by

$$\Gamma_{\text{azo},0} = \frac{d_{\text{PCLM}} \rho_{\text{PCLM}} k}{M_{n,\text{PCLM}}} \quad (13)$$

where ρ_{PCLM} is the initiator density, k is the number of repeat units in the initiator (Figure 2), and $M_{n,\text{PCLM}}$ is its number-average molecular weight. Thus, the initial density was given as $\Gamma_{\text{azo},0} = 1.1 \times 10^{-6}$ mol/m² for evaporated SiO_x and $\Gamma_{\text{azo},0} = 3.7 \times 10^{-7}$ mol/m² for polished silicon wafers.

“Grafting-From” Polymerization. Methyl, *n*-butyl, *n*-hexyl, lauryl, and stearyl methacrylate were chosen as monomers for the surface polymerizations to adjust the polarity of the monolayers. Decalin was chosen as a solvent for the surface polymerizations since it is a solvent for the corresponding polymers and a nonsolvent for the initiator. The only exception in this series was the polymerization of methyl methacrylate where toluene, which is a good solvent for poly(methyl methacrylate), was chosen since no solvent was found which dissolved poly(methyl methacrylate) but not the initiator. Because dissolution of the initiator during the polymerization process might be a potential problem, the solubility of the poly(ϵ -caprolactone)diol in monomer/solvent mixtures at 60 °C was tested. This is important since some of the bulk monomers are solvents for the macroinitiator. The mixture methyl methacrylate/toluene turned out to be a solvent for the initiator at any ratio. Thus, a volume ratio of 1:1 was chosen. The maximum monomer concentration in *n*-alkyl methacrylate/decalin mixtures still keeping the poly(ϵ -caprolactone)diol in nonsolvent conditions was determined by turbidity measurements. It was observed that the poly(ϵ -caprolactone)diol was insoluble if the monomer concentration was chosen below 37 vol % for *n*-butyl methacrylate or below 44 vol % for *n*-hexyl methacrylate. The pure monomers lauryl and stearyl methacrylate turned out to be nonsolvents for the poly(ϵ -caprolactone)diol. Accordingly, all polymerization reactions were carried out using a *n*-alkyl methacrylate/decalin volume ratio of 1:2.

After completion of the polymerization process, removal of only loosely attached homopolymer is an important issue. Nonbonded homopolymer can for example result from transfer reactions of a grafted growing polymer chain to monomer or solvent or thermal polymerization in solution. Therefore, all substrates were carefully extracted in a continuous extraction setup. The poly(*n*-alkyl methacrylate)-covered samples were extracted for 16 h with cyclohexane, which is a nonsolvent for the initiator and a solvent for the poly(*n*-alkyl methacrylate)s. After an initial period in which loosely adhering homopolymer was removed, no further polymer could be extracted from the layer and a constant thickness was observed. Exceptions to this were the poly(methyl methacrylate)-covered samples. As already mentioned above, no solvent could be found that is a solvent for poly(methyl methacrylate) and a nonsolvent for the initiator. Accordingly, the extractions were carried out in toluene. During extraction a slow continuous decrease in the film thickness was observed. Reproducible values were only observed if a continuous extraction time, e.g. 16 h, was applied. Such an extraction time is known to be sufficient³⁶ to remove all weakly attached poly(methyl methacrylate) homopolymer. In this case the free energy of solvation of the block copolymer is apparently high enough to overcome the free energy of adsorption.

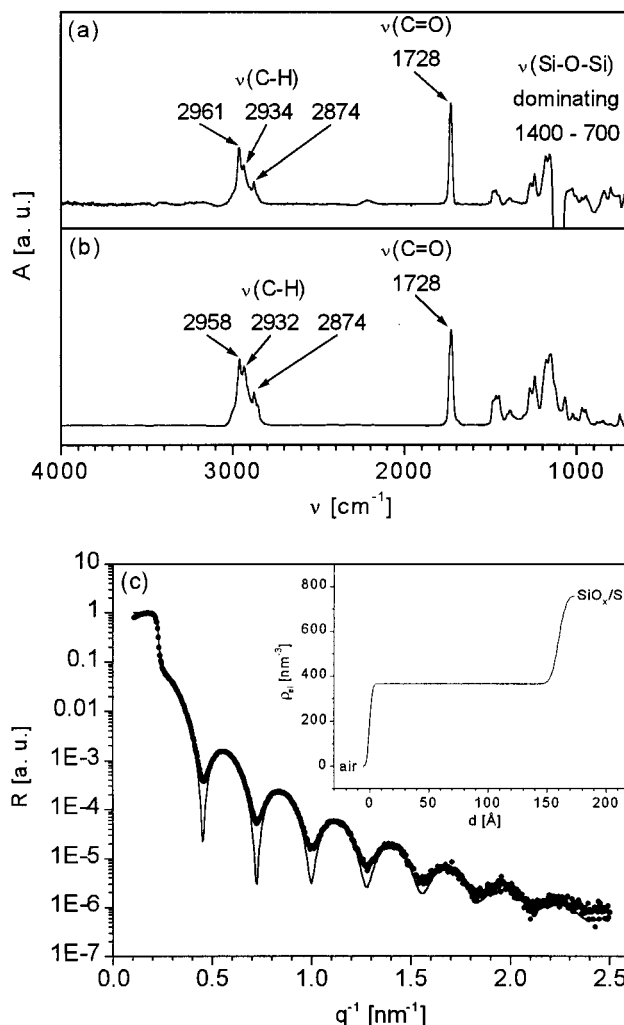


Figure 9. (a) Transmission IR spectrum of a poly(ϵ -caprolactone)-block-poly(*n*-butyl methacrylate) monolayer. The layer thickness of $d_{\text{PnBMA}} = 225$ Å on both faces of the sample was determined by ellipsometry. For comparison, the IR spectrum of the bulk polymer is shown in (b). (c) X-ray reflectivity curve of a $d_{\text{PnBMA}} = 157$ Å thick monolayer of the same polymer (thickness by ellipsometry $d_{\text{PnBMA}} = 160$ Å). The inset indicates the profile of the electron density ρ_{el} . Substrate Si/SiO_x: $\rho_{\text{el}} = 736$ nm⁻³, $\sigma = 0.65$ nm. Poly(ϵ -caprolactone)-block-poly(*n*-butyl methacrylate) layer: $\rho_{\text{el}} = 366$ nm⁻³, $\sigma = 0.19$ nm.

The poly(ϵ -caprolactone) macroinitiator physisorbed to silicon oxide was used to start the radical chain polymerization of the *n*-alkyl methacrylates. Since there are about five azo groups in each adsorbed initiator chain, the successful initiation of for example one central azo group leads to two diblock copolymers. The initiation by a terminal azo group would lead to a diblock copolymer and a free homopolymer, which is washed out during extraction. If the two freshly generated initiator radicals are kept in the solvent cage and react by recombination, the anchor block will simply be extended (Figure 5).

The bulk refractive indices $n_D^{20} = 1.4893$ for poly(methyl methacrylate),³⁷ 1.4830 for poly(*n*-butyl methacrylate),³⁷ 1.4813 for poly(*n*-hexyl methacrylate),³⁷ and 1.4740 for poly(lauryl methacrylate)³⁷ were used to evaluate data obtained by surface plasmon spectroscopy and ellipsometry. The refractive index $n_D^{20} = 1.4711$ of poly(stearyl methacrylate) was determined by extrapo-

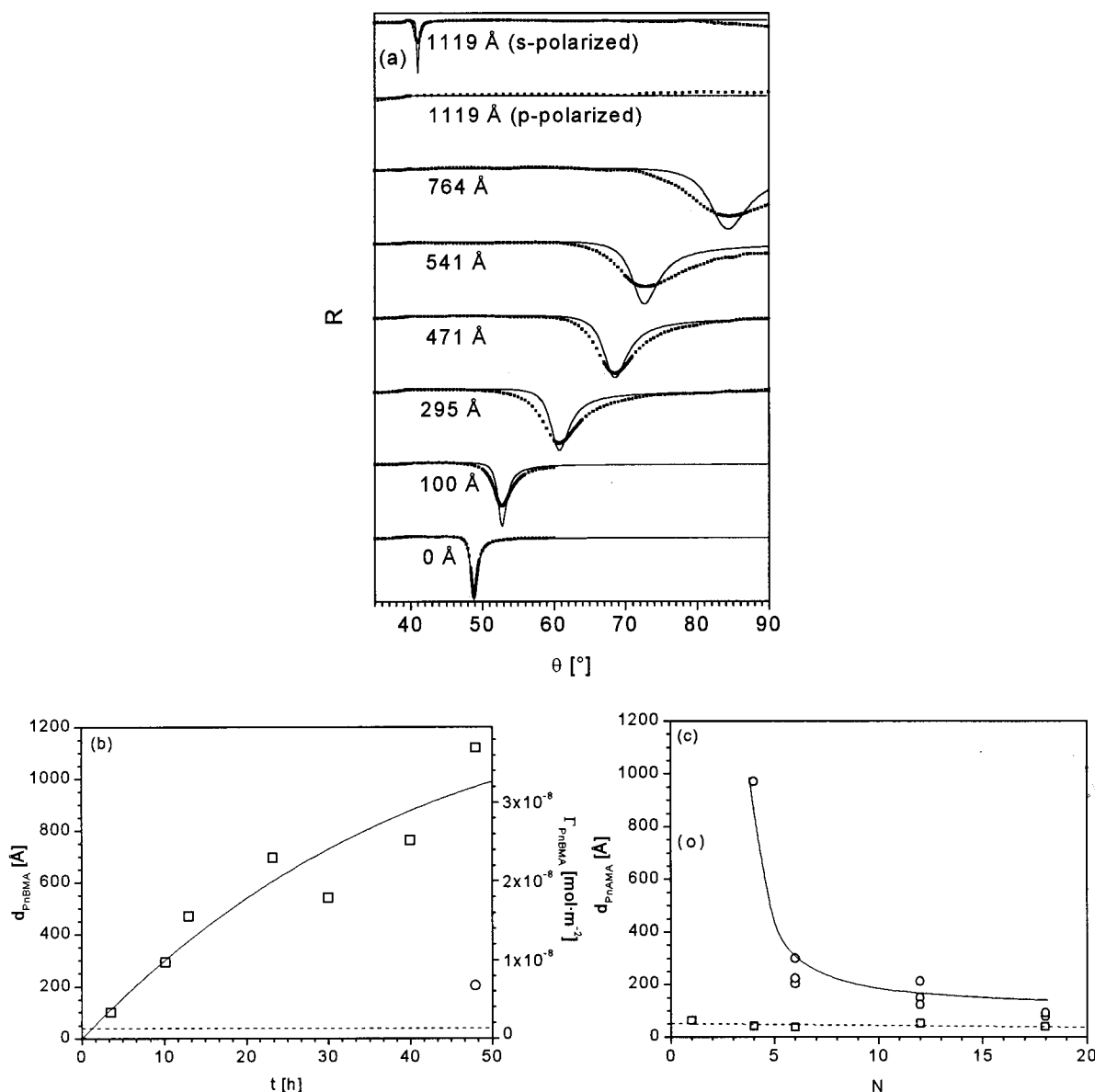


Figure 10. (a) Reflectivity curves of selected poly(ϵ -caprolactone)-*block*-poly(*n*-butyl methacrylate) monolayers ordered by increasing polymerization time (0, 3.5, 10.2, 13, 30, 40, 48 h). Solid lines are fitted reflectivity curves according to Fresnel equations. (b) Time dependence of the buoy block layer thickness d_{PnBMA} and the corresponding graft density Γ_{PnBMA} (\square). Additionally, the value obtained using polished silicon wafers is given (\circ). The solid line describes the calculated thickness $d_{\text{PnBMA}}(t)$ according to eq 17. The dashed line reflects a reference obtained on substrate without adsorbed initiator after 48 h of "polymerization". (c) Dependence of the film thickness on the side chain length N (polymerization time $t = 48$ h) (\circ). The dashed line reflects corresponding reference experiments without initiator (\square) after 48 h of "polymerization".

lation of the refractive indices of the polymers with the shorter side chain.

First experiments were performed by polymerizing *n*-butyl methacrylate for 48 h onto polished silicon wafers having adsorbed initiator monolayers. The IR spectra shown in Figure 9a,b prove the monolayer formation. Good agreement is observed between the transmission FTIR spectrum taken for a monolayer of poly(*n*-butyl methacrylate) and the FTIR spectrum of a cast film. That the samples are covered by a homogeneous, relatively smooth polymer layer can be concluded from X-ray reflectometry measurements. In Figure 9c the reflectometry curve of a poly(*n*-butyl methacrylate) monolayer and the determined parameters are given. The obtained electron density of the poly(*n*-butyl methacrylate) layer $\rho_{\text{el}} = 366 \text{ nm}^{-3}$ equals a density of 1.10 g/cm^3 , which is close to the bulk density of 1.055 g/cm^3 ,²⁸

indicating a similar chain packing as in the bulk. An average thickness of $d_{\text{PnBMA}} = 205 \pm 79 \text{ Å}$ was obtained from several ellipsometry and X-ray reflectometry measurements on samples polymerized under the conditions described above.

Samples for surface plasmon spectroscopy having initiator layers adsorbed to evaporated SiO_x were taken after selected polymerization times t , and the reflectivity curves were recorded (Figure 10a). It is shown that the poly(*n*-butyl methacrylate) layer thickness d_{PnBMA} can easily be adjusted up to 1000 Å (Figure 10b). With increasing side chain length N of the monomer the poly(*n*-alkyl methacrylate) layer thickness d_{PnBMA} is strongly reduced (Figure 10c). The thicknesses d_{PnBMA} on evaporated SiO_x is significantly higher than on polished silicon wafers (Figure 10b). This agrees nicely with the difference in the macroinitiator layer thickness d_{PCLM}

which has been attributed to the difference in substrate roughness.

The increase in film thickness with increasing polymerization time (Figure 10b) can be described using the standard kinetic model for the free radical chain polymerization. If the azo decomposition process is considered to be a first-order reaction, the surface density of decomposed azo groups $\Gamma_{\text{dec,azo}}(t)$ is given by

$$\Gamma_{\text{dec,azo}}(t) = \Gamma_{\text{azo},0}(1 - \exp(-k_D t)) \quad (14)$$

where $\Gamma_{\text{azo},0}$ is the initial azo surface density and k_D is the rate constant of the thermal decomposition process, as determined above. The graft density of the poly(*n*-alkyl methacrylate) blocks as a function of time $\Gamma_{\text{PnAMA}}(t)$ can easily be calculated according to

$$\Gamma_{\text{PnAMA}}(t) = \frac{d_{\text{PnAMA}}(t)\rho_{\text{PnAMA}}}{M_{n,\text{PnAMA}}} \quad (15)$$

where ρ_{PnAMA} is the density and $M_{n,\text{PnAMA}}$ is the number-average molecular weight of the surface-attached poly(*n*-alkyl methacrylate) blocks. The densities ρ_{PnAMA} can be assumed to be similar to the bulk densities (1.17 g/cm³ for methyl,³⁸ 1.055 g/cm³ for *n*-butyl,³⁸ 1.01 g/cm³ for *n*-hexyl,³⁸ and 0.929 g/cm³ for lauryl methacrylate³⁸). A value of 0.901 g/cm³ for stearyl methacrylate was estimated by extrapolation of the densities of the polymers with the shorter side chain.

The molecular weight $M_{n,\text{PnAMA}}$ does not depend on the polymerization time since the monomer concentration during the surface polymerization process remains practically constant.²⁹ The molecular weight of the surface-attached chains can be inferred from the molecular weight of the free polymer formed during the polymerization process. It has been shown for the radical "grafting-from" polymerization of methyl methacrylate in toluene using monolayers of initiators self-assembled onto planar surfaces that the molecular weight of the surface attached chains is practically identical to the molecular weight of the chains formed in solution.³⁶ Free polymer originates for example from transfer reactions of a grafted growing polymer chain to monomer or solvent or thermal polymerization. SEC measurements of the free poly(*n*-alkyl methacrylate) showed that very high molecular weight polymers had been formed. A typical SEC trace of a poly(*n*-butyl methacrylate) sample is depicted in Figure 11a. In all cases the number-average molecular weights $M_{n,\text{PnAMA}}$ were around $(2-3) \times 10^6$ g/mol, and the polydispersities D were around 2.0–2.5. This agrees with results of Buback and co-workers,³⁹ who determined similar molecular weights if *n*-butyl and lauryl methacrylate were polymerized under identical conditions. A slight decrease of the apparent $M_{n,\text{PnAMA}}$ and $M_{w,\text{PnAMA}}$ toward higher chain lengths N is observed (Figure 11b). This can be explained by a slightly decreasing monomer concentration due to decreasing monomer densities⁴⁰ and increasing molecular weights of the monomers toward higher side chain lengths N . Additionally, for some samples the weight-average molecular weights $M_{w,\text{PnAMA}}$ were determined by static light scattering. The obtained values confirm the very high molecular weights measured by SEC and the trend of decreasing molecular weights with increasing length of the side chains N . The $M_{w,\text{PnAMA}}$ values obtained by SEC measurements are systematically about 30% smaller than those obtained

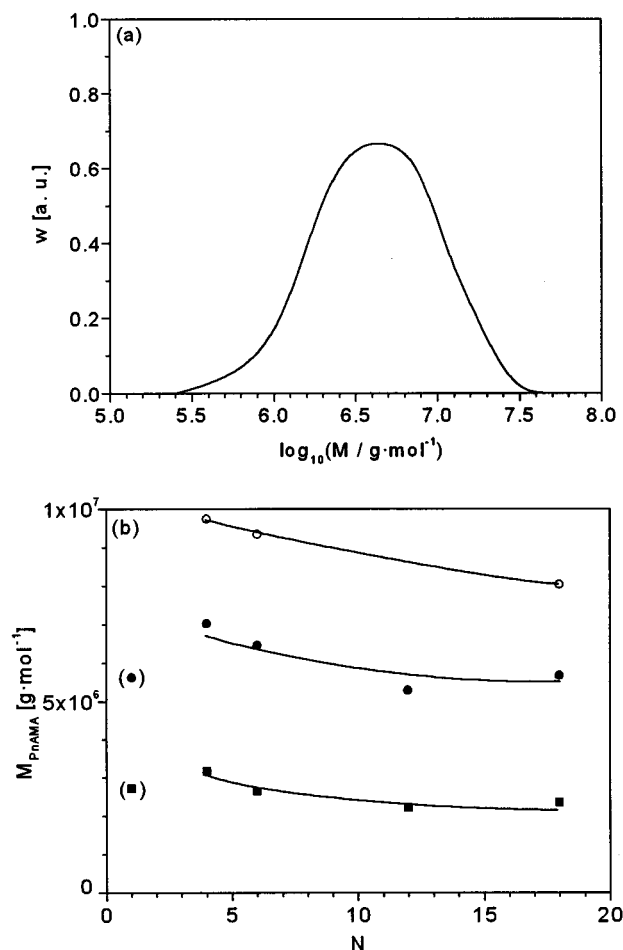


Figure 11. (a) SEC trace of a sample of nonattached poly(*n*-butyl methacrylate); apparent $M_{n,\text{PnBMA}} = 3.1 \times 10^6$ g/mol and $D = 2.1$. (b) Number-average $M_{n,\text{PnAMA}}$ (■) and weight-average $M_{w,\text{PnAMA}}$ (●) determined by SEC using a poly(methyl methacrylate) calibration and weight-average $M_{w,\text{PnAMA}}$ (○) determined by static light scattering vs side chain length N .

by static light scattering. This, among other factors, might be explained by a slightly deviating SEC calibration, since a considerable amount of polymer (Figure 11a) has a molecular weight higher than the highest molecular weight standard used (1.35×10^7 g/mol after universal calibration). However, as the number-average molecular weight $M_{n,\text{PnAMA}}$ obtained by SEC should be less affected by such calibration errors, the graft densities of poly(*n*-alkyl methacrylate) Γ_{PnAMA} could be estimated according to eq 15 with sufficient precision. In Figure 10b the thicknesses d_{PnBMA} of the polymer films are shown as a function of the graft density Γ_{PnBMA} of the surface-attached chains.

The radical efficiency factor $f(t)$ for surface polymerization processes is defined analogous to the efficiency in bulk polymerizations:²⁹

$$f(t) = \frac{\Gamma_{\text{PnAMA}}(t)}{\Gamma_{\text{dec,azo}}(t)} \quad (16)$$

For the evaluation of the radical efficiency factor, it has to be considered that this factor does not remain constant during the polymerization reaction but is usually a strong function of the conversion. The radical efficiency factor for the surface polymerization of *n*-butyl methacrylate is depicted as a function of the polymerization time in Figure 12a. It can be seen that $f(t)$

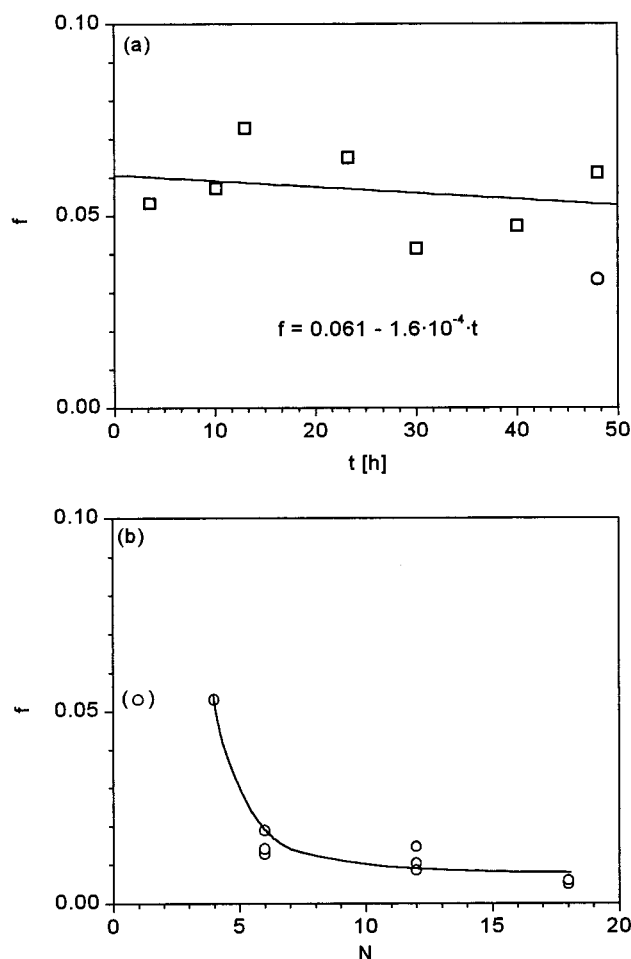


Figure 12. (a) Time dependence of the radical efficiency factor f for the surface polymerization of *n*-butyl methacrylate using wafers bearing evaporated SiO_x (□). Data were fitted using a simple linear model. Additionally, the efficiency f for the same process on polished silicon wafers (○) is shown. (b) Dependence of the radical efficiency of the polymerization process on the side chain length N (polymerization time $t = 48$ h) (○).

slightly decreases from 0.06 in the beginning to 0.05 at the end of the polymerization reaction where about 50% of the azo groups have been decomposed. A decrease of the efficiency with increasing conversion has already been described for other radical surface¹⁸ and bulk²⁹ polymerizations. This is most likely due to a viscosity increase in the polymer monolayer with increasing conversion. It can be seen that the efficiency f of a macroinitiator monolayer obtained on polished silicon wafers is in the same range as for substrates having evaporated SiO_x layers on top although the absolute values of the film thickness are significantly different. Additionally, Figure 12b shows that the efficiency f decreases rapidly with increasing side chain length N of the monomer. This agrees with the general trend observed for polymerization in solution, where the radical efficiency factor is known to vary for different monomers as a consequence of the relative rates with which initiator radicals add to different monomers.²⁹ It should be noted that all the obtained values for f (Figure 12a,b) are well below typical values known for the bulk ($f = 0.3$ – 0.8 ²⁹) and surface ($f = 0.3$ ¹⁸) polymerization of methyl methacrylate using AIBN-like initiators. The reason for this difference could be the fact that both sides of nearly every azo moiety are bonded to polymer chains that are strongly adsorbed to the surface. Thus,

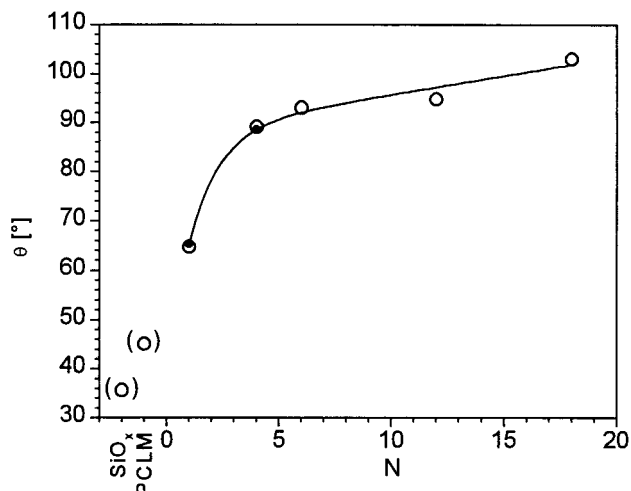


Figure 13. Sessile contact angles (○) for poly(ε-caprolactone)-block-poly(*n*-alkyl methacrylate) monolayers of increasing side chain length N . In addition, the reference values for silicon oxide (SiO_x) and the poly(ε-caprolactone) macroinitiator (PCLM) are given. In the case of $N = 1$ and $N = 4$ also the contact angles measured on thinner films (~ 200 Å) are shown (●).

it can easily be envisioned that it is considerably more difficult for the two radicals obtained after azo decomposition to diffuse out of the solvent/monomer cage and to successfully start a polymerization reaction than for free initiator in solution and for initiator attached by one end at the substrate surface.¹⁸

After determination of the radical efficiency factor $f(t)$ the layer thickness $d_{\text{PnAMA}}(t)$ can be calculated combining eqs 14–16:

$$d_{\text{PnAMA}}(t) = \frac{\Gamma_{\text{azo},0} M_{\text{n,PnAMA}}}{\rho_{\text{PnAMA}}} f(t) (1 - \exp(-k_D t)) \quad (17)$$

The expected thickness dependence of the polymer monolayer $d_{\text{PnBMA}}(t)$ calculated according to eq 17 is depicted in Figure 10b. The good agreement between the measured thickness values and the kinetic model shows that the growth of the polymer layer can be easily controlled.

The macroinitiator approach described above can be used to tailor the surface properties of monolayers by polymerizing a monomer of specifically chosen hydrophilicity or hydrophobicity. Water contact angle measurements show a strong decrease of the surface polarity with increasing length of the alkyl side chain N (Figure 13). The contact angle (sessile drop) for the unmodified silicon oxide was 36° . This value is changed to 45° after physisorption of the poly(ε-caprolactone) macroinitiator. Through attachment of the poly(*n*-alkyl methacrylate) blocks the contact angle can be controlled from 65° for poly(methyl methacrylate) to 103° for poly(stearyl methacrylate) due to the increasing length of the nonpolar aliphatic side chain. The obtained contact angles for the molecularly thin polymer films are in close agreement with those of cast poly(*n*-alkyl methacrylate) films.^{41,42}

Conclusions

The macroinitiator concept allows the creation of block copolymers of different polarities at solid surfaces in situ. In this study block copolymers consisting of a hydrophilic anchor block (poly(ε-caprolactone)) and a hydrophobic buoy block (poly(*n*-alkyl methacrylate)) were generated at hydrophilic surfaces (silicon oxide).

The poly(ϵ -caprolactone) macroinitiator shows a thermal decomposition behavior similar to AIBN and can reproducibly be physisorbed to silicon oxide surfaces. The macroinitiator concept allows to tether buoy blocks of very high molecular weights to the substrate surface by a relatively short anchor block. In the example shown here block copolymers with buoy block molecular weights $M_{n,PnAMA}$ of $(2-3) \times 10^6$ g/mol were attached to the surface with distances between the anchor points down to 70 Å. The resulting monolayers had dry film thicknesses, which in some cases exceeded 1000 Å. The thickness of the block copolymer layers can easily be controlled for example by adjusting the polymerization time. Good agreement between the measured values and those calculated using a standard model for radical chain polymerization is observed.

An upper limit for the film thickness, which can be obtained using polymeric macroinitiators, is given by the low radical efficiency factor ($f \approx 0.05$) of such a system due to the slow diffusion of the initiator radicals out of the solvent cage. However, it should be noted that the layer thicknesses obtained by the macroinitiator approach are still more than an order of magnitude higher than those values obtained by block copolymer adsorption which are typically limited to values below 50 Å.

Solubility problems which are a major limitation of any block copolymer physisorption process can be avoided by growing the polymer directly at the surface of the substrate in situ. Since the buoy block is generated in a separate step, no common solvent of the block copolymer has to be found. Indeed, it is even detrimental if buoy block and anchor block have similar dissolution properties, as the poly(methyl methacrylate)/poly(ϵ -caprolactone) example has shown. Under such conditions the block copolymer can be removed partly or completely during prolonged extraction. In contrast to this, systems with strongly differing solution properties of anchor and buoy block are stable, even after many hours of solvent exposure.

The direct generation of block copolymer monolayers at the surface of a substrate allows to influence the surface polarity of a material strongly and to tune it to a desired value. Through the growth of surface-attached block copolymer monolayers having a buoy block which consists of a statistical copolymer a precise tailoring of the surface properties can be achieved. In conclusion, it can be stated that the macroinitiator route seems to be a promising approach for the anchoring of polymer molecules to solid surfaces. Such a strategy for the deposition of polymer monolayers might offer new perspectives for the surface modification of materials.

Acknowledgment. Will Shen and Ralf K  gler are thanked for measuring and fitting the X-ray data. Financial support under the BMBF grant "Innovative Methoden der Polymercharakterisierung f  r die Praxis" (Nr. 03N6010) and by Schott Glas is gratefully acknowledged.

References and Notes

- (1) Dorgan, J. R.; Stamm, M.; Toprakcioglu, C.; J  r  me, R.; Fetters, L. J. *Macromolecules* **1993**, *26*, 5321.
- (2) Guzonas, D. A.; Boils, D.; Tripp, C. P.; Hair, M. L. *Macromolecules* **1992**, *25*, 2434.
- (3) Field, J. B.; Toprakcioglu, C.; Ball, R. C.; Stanley, H. B.; Dai, L.; Barford, W.; Penfold, J.; Smith, G.; Hamilton, W. *Macromolecules* **1992**, *25*, 434.
- (4) Motschmann, M.; Stamm, M.; Toprahcioglu, C. *Macromolecules* **1991**, *24*, 3681.
- (5) Kelley, T. W.; Schorr, P. A.; Johnson, K. D.; Tirrell, M.; Frisbie, C. D. *Macromolecules* **1998**, *31*, 4297.
- (6) Belder, G. F.; ten Brinke, G.; Hadzioannou, G. *Langmuir* **1997**, *13*, 4102.
- (7) Meiners, J. C.; Ritz, A.; Rafailovich, M. H.; Sokolov, J.; Mlynek, J.; Krausch, G. *Appl. Phys. A* **1995**, *61*, 519.
- (8) Parsonage, E.; Tirrell, M.; Watanabe, H.; Nuzzo, R. G. *Macromolecules* **1991**, *24*, 1987.
- (9) Ding, J.; Tao, J.; Guo, A.; Stewart, S.; Hu, N.; Birss, V. I.; Liu, G. *Macromolecules* **1996**, *29*, 5398.
- (10) Amiel, C.; Sikka, M.; Schneider, J. W.; Tsao, Y.-H.; Tirrell, M.; Mays, J. W. *Macromolecules* **1995**, *28*, 3125.
- (11) Wu, D. T.; Yokoyama, A.; Setterquist, R. L. *Polym. J.* **1991**, *23*, 1991.
- (12) Fleer, G. J.; Cohen Stuart, M. A.; Scheutjens, J. M. H. M.; Cosgrove, T.; Vincent, B. *Polymers at Interfaces*; Chapman & Hall: London, 1993; Chapter 6.
- (13) Russell, T. P. *Curr. Opin. Colloid Interface Sci.* **1996**, *1*, 107.
- (14) Kopf, A.; Baschnagel, J.; Wittmer, J.; Binder, K. *Macromolecules* **1996**, *29*, 1433.
- (15) Zajac, R.; Chakrabarti, A. *Phys. Rev. B* **1995**, *52*, 6036.
- (16) Boven, G.; Oosterling, M. L. C. M.; Challa, G.; Schouten, A. J. *Polymer* **1990**, *31*, 2377.
- (17) Prucker, O.; R  he, J. *Macromolecules* **1998**, *31*, 592.
- (18) Prucker, O.; R  he, J. *Macromolecules* **1998**, *31*, 602.
- (19) Korn, M.; Killmann, E. *J. Colloid Interface Sci.* **1980**, *76*, 19.
- (20) Killmann, E.; Korn, M.; Bergmann, M. In *Adsorption from Solution*; Academic Press: London, 1983.
- (21) Felter, R. E. *J. Polym. Sci., Polym. Lett. Ed.* **1974**, *12*, 147.
- (22) Prucker, O. Ph.D. Thesis, University of Bayreuth, Germany, 1995.
- (23) Kurata, M.; Tsunashima, Y. In *Polymer Handbook*, 3rd ed.; Brandrup, J., Immergut, E. H., Eds.; John Wiley & Sons: New York, 1989; Chapter VII.
- (24) Wads  , I. In *Principles of Medical Biology*; JAI Press: London, 1996; Vol. 4., Part III, Chapter 10.
- (25) Hill, J. O.;   jelund, G.; Wads  , I. *J. Chem. Thermodyn.* **1969**, *1*, 111.
- (26) Kretschmann, E. *Opt. Commun.* **1972**, *6*, 185.
- (27) Forster, M. *Vacuum* **1990**, *41*, 1441.
- (28) Lekner, J. *Theory of Reflection of Electromagnetic and Particle Waves*; M. Nijhoff Publishers: Dordrecht, 1987.
- (29) Odian, G. *Principles of Polymerization*, 3rd ed.; John Wiley & Sons: New York, 1991; Chapter 3.
- (30) Meier, L. P.; Shelden, R. A.; Caseri, W. R.; Suter, U. W. *Macromolecules* **1994**, *27*, 1637.
- (31) Boven, G.; Oosterling, M. L. C. M.; Challa, G.; Schouten, A. J. *Polymer* **1990**, *31*, 2377.
- (32) Nuyken, O.; Gerum, J.; Steinhausen, R. *Makromol. Chem.* **1979**, *180*, 1497.
- (33) Torfs, J. C. M.; Deij, L.; Dorrepaal, A. J.; Heijens, J. C. *Anal. Chem.* **1984**, *56*, 2863.
- (34) Starnes, W. H.; Plitz, I. M.; Schilling, F. C.; Villacorta, G. M.; Park, G. S.; Saremi, A. H. *Macromolecules* **1984**, *17*, 2507.
- (35) Masson, J. C. In *Polymer Handbook*, 3rd ed.; Brandrup, J., Immergut, E. H., Eds.; John Wiley & Sons: New York, 1989; Chapter II.
- (36) Schimmel, M. Ph.D. Thesis, Johannes-Gutenberg Universit  t Mainz, Germany, 1997.
- (37) Seferis, J. C. In *Polymer Handbook*, 3rd ed.; Brandrup, J., Immergut, E. H., Eds.; John Wiley & Sons: New York, 1989; Chapter VI.
- (38) Van Krevelen, D. W. *Properties of Polymers*; Elsevier: Amsterdam, 1997.
- (39) Buback, M.; Geers, U.; Kurz, C. U. *Macromol. Chem. Phys.* **1997**, *198*, 3451.
- (40) Riddle, E. H. *Monomeric Acrylic Esters*; Reinhold Publishing: New York, 1954.
- (41) Kamagata, K.; Toyama, M. *J. Appl. Polym. Sci.* **1974**, *18*, 167.
- (42) Park, I.-J. Ph.D. Thesis, Seoul National University, Seoul, Korea, 1996.